

AD-A112 174

AERONAUTICAL RESEARCH LABS MELBOURNE (AUSTRALIA)

F/G 20/11

THE SIMULATION OF LOCAL STRESS-STRAIN BEHAVIOUR WITH APPLICATION--ETC(U)

JUL 79 R C FRASER

UNCLASSIFIED

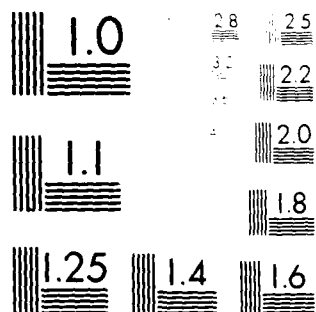
ARL/STRUC-385

NL

1 OF 1
413-A
11-21-74

END
DATE
FILMED

04-82
DTIC



MODERNITY RESOLUTION TEST CHART
NBS 1010-A-10



AD A112174

DEPARTMENT OF DEFENCE
DEFENCE SCIENCE AND TECHNOLOGY ORGANISATION
AERONAUTICAL RESEARCH LABORATORIES

MELBOURNE, VICTORIA

STRUCTURES REPORT 385

THE SIMULATION OF LOCAL STRESS-STRAIN
BEHAVIOUR WITH APPLICATION TO FATIGUE
ANALYSIS

by

R. C. FRASER

Approved for Public Release.



© COMMONWEALTH OF AUSTRALIA 1981

COPY No 1

JULY, 1979

014

120
DTC
MAR 19 1982
H

DTC FILE COPY

DEPARTMENT OF DEFENCE
DEFENCE SCIENCE AND TECHNOLOGY ORGANISATION
AERONAUTICAL RESEARCH LABORATORIES

STRUCTURES REPORT 385

**THE SIMULATION OF LOCAL STRESS-STRAIN
BEHAVIOUR WITH APPLICATION TO FATIGUE
ANALYSIS**

by

R. C. FRASER

DTIC
1982

SUMMARY

Substantial improvement in fatigue life prediction has been effected by the introduction of cyclic stress-strain concepts. A procedure that incorporates these in a simulation of local stress and strain from nominal load using Neuber notch analysis is described in relation to its application to the fatigue analysis of in-service load histories.

In the present simulation the non-linear stress-strain and Neuber equations are solved numerically rather than by piecewise approximations. For the long load histories occurring in practice this improves numerical stability.

DOCUMENT CONTROL DATA SHEET

Security classification of this page: Unclassified

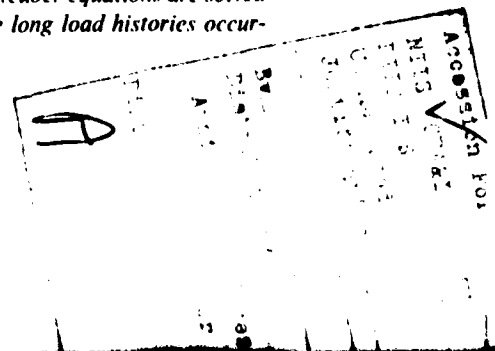
1. Document Numbers (a) AR Number: AR-002-247 (b) Document Series and Number: Structures Report 385 (c) Report Number: ARL-Struc-Report-385	2. Security Classification (a) Complete document: Unclassified (b) Title in isolation: Unclassified (c) Summary in isolation: Unclassified									
3. Title: THE SIMULATION OF LOCAL STRESS STRAIN BEHAVIOUR WITH APPLICATION TO FATIGUE ANALYSIS										
4. Personal Author(s): R. C. Fraser	5. Document Date: July, 1979									
6. Type of Report and Period Covered:										
7. Corporate Author(s): Aeronautical Research Laboratories	8. Reference Numbers (a) Task: 7615/156 (b) Sponsoring Agency:									
9. Cost Code: 27 7030										
10. Imprint Aeronautical Research Laboratories, Melbourne	11. Computer Program(s) (Title(s) and language(s)):									
12. Release Limitations (of the document): Approved for public release.										
<table border="1"> <tr> <td>12.0. Overseas:</td> <td>N.O.</td> <td>P.R.</td> <td>I</td> <td>A</td> <td>B</td> <td>C</td> <td>D</td> <td>E</td> </tr> </table>		12.0. Overseas:	N.O.	P.R.	I	A	B	C	D	E
12.0. Overseas:	N.O.	P.R.	I	A	B	C	D	E		
13. Announcement Limitations (of the information on this page): No Limitation										
14. Descriptors: Fatigue life Stress concentration Predictions Notch tests	15. Cosati Codes: 1113 2012									

16.

ABSTRACT

Substantial improvement in fatigue life prediction has been effected by the introduction of cyclic stress-strain concepts. A procedure that incorporates these in a simulation of local stress and strain from nominal load using Neuber notch analysis is described in relation to its application to the fatigue analysis of in-service histories.

In the present simulation the non-linear stress-strain and Neuber equations are solved numerically rather than by piecewise approximations. For the long load histories occurring in practice this improves numerical stability.



CONTENTS

	Page No.
1. INTRODUCTION	1
2. CYCLIC STRESS-STRAIN CONCEPTS	1
2.1 Memory	7
2.2 Cyclic Relaxation and Creep	7
3. NEUBER NOTCH ANALYSIS	7
4. SIMULATION OF LOCAL STRESS-STRAIN	10
4.1 Present Method	10
4.1.1 Relaxation	10
4.1.2 Modelling	10
4.1.3 Numerical Methods	12
4.2 Miscellaneous Effects	14
5. CALCULATION OF FATIGUE DAMAGE	15
6. CONCLUSIONS	15
REFERENCES	
APPENDIX—Computer Simulation of Local Stress-Strain	
DISTRIBUTION	

1. INTRODUCTION

Expressed simplistically, the economic design of a modern metallic structure often dictates that it operates with a minimum amount of material for a substantial life. The former requirement is usually determined by such factors as capital cost, size or weight constraints, while the latter is determined by the need to maximise the gains for which the structure was designed. However, there exists a fundamental conflict between these two design objectives in that the former inevitably raises peak stresses and strains while forcing down the life of the structure. The trade-off between the two has received much attention in recent years not only in relation to design but also in response to a need to re-evaluate the condition of old structures that are being called upon to last longer than originally anticipated.

In the literature various methods have been developed recently to enable one to account for the effects of peak stresses and strains on fatigue life. Of these a technique originally proposed by Neuber¹ for static loading but developed by Topper *et al.*² has obtained unique importance for fatigue. Based on the notch analysis of shear strained prisms the method allows the determination of stresses and strains local to a specific stress raiser using information on the nominal stress-strain state of the member in question in conjunction with data detailing the response of the metal to cyclic plasticity.

Two distinct approaches to the analysis of fatigue life using Neuber analysis have emerged. Topper *et al.*², Morrow *et al.*³ and Wetzel⁴ have analysed successfully the fatigue behaviour of notched structures by using Neuber analysis to control the loading of appropriate smooth specimens. Other researchers⁵⁻⁹ however, have studied the fatigue behaviour of various structures by using Neuber analysis to simulate the stress-strain state local to critical stress raisers. The fundamental difference between the two approaches is that whereas the latter must use empirical relations describing the stress-strain and damage response of the material to cyclic load, the former utilises an "exact" representation of this information - the specimen.

However, the advantages in terms of cost, time and flexibility of a computer simulation over a laboratory simulation of local stress-strain cum fatigue behaviour is such that it is likely to be used increasingly in the future for the life analysis of both new and old structures.

The present paper describes the initial development of a computer program written in PASCAL that is designed to predict the life of structures under in-service load histories. The advantage of this program is that the non-linear model equations are solved directly without further approximation of the stress-strain equations. Over a long sequence this improves numerical stability for a surprisingly small computing cost.

2. CYCLIC STRESS-STRAIN CONCEPTS

As a background this section and the next summarise the salient, well known features of local plasticity in fatigue.^{10,11,12}

The inelastic response of metals to cyclic load can be complex as demonstrated in Figure 1 and involves the simultaneous interaction of stress-strain hysteresis or memory, cyclic softening or hardening and the relocation of mean stress through cyclic creep. Of these, hysteresis is the most obvious and important and can be defined simply as a lack of reversibility when a given stress-strain state or path moves towards a tension or compression. Figure 2 depicts the response of a metal at a stress raiser to a completely reversed loading, and it can be seen that the local stress-strain state moves along two distinct paths when cycling to or from either the compressive or tensile situations, i.e. the local stress-strain path does not retrace its movement when cycling to or from a given state. The initial hysteresis loop that is evident in Figure 2 does not represent a stable condition in most practical instances and will alter as shown in Figure 3 upon application of further load cycles; when the strain change per stress change for each reversal

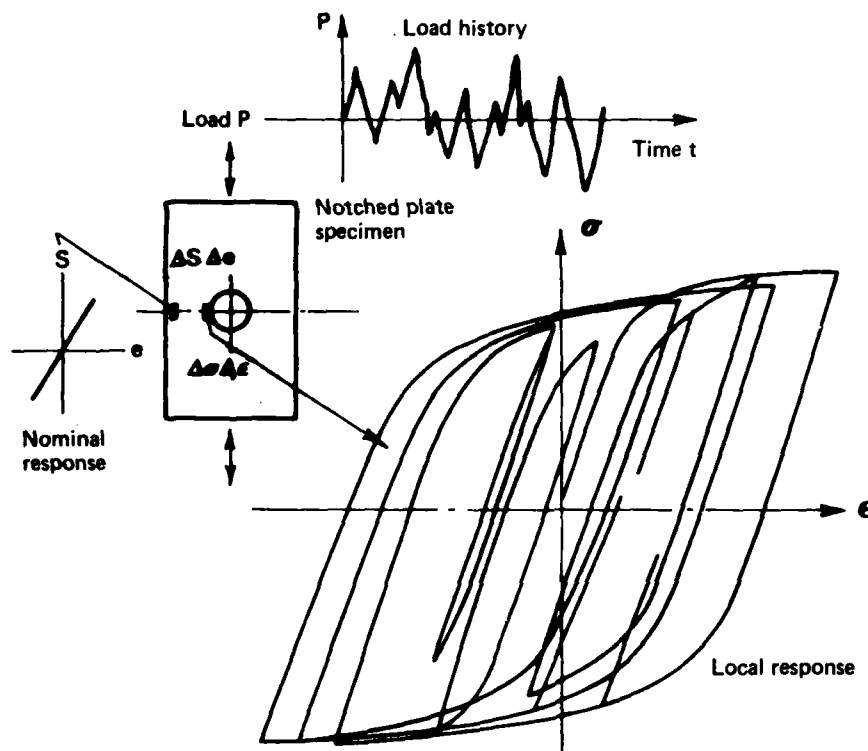


FIG. 1 REPRESENTATION OF NOMINAL AND LOCAL STRESS - STRAIN BEHAVIOUR AT A STRESS RAISER DURING A COMPLEX LOADING SEQUENCE

is decreasing locally then the material is said to cyclically harden and vice-versa for cyclical softening. For most materials, after many cycles, the hysteresis loop will eventually stabilize, and by plotting the locus of tips of stable hysteresis loops from companion tests conducted at different amplitudes of local reversed stress (or strain) one obtains a steady state stress-strain curve of amplitude. This is analogous to and can be compared with the usual monotonic stress-strain curve—see Figure 4. Cyclically induced changes are immediately evident by such comparisons as shown in Figure 5. A metal that cyclically hardens will have a cyclic stress-strain curve (as the locus of stable hysteresis loop tips is called) above the monotonic curve and conversely if the cyclic curve is below the monotonic curve the metal cyclically softens.

Hardening and softening are usually transient phenomena that occur early in the fatigue life of a metal, often quite rapidly* (see Section 2.2). This frequently permits simulation of fatigue using only the steady state properties without affecting life predictions significantly. The determination of cyclic stress-strain curves using fast incremental step strain tests is described in

* Typically, softening occupies 30% of total life while hardening is complete after 1%.

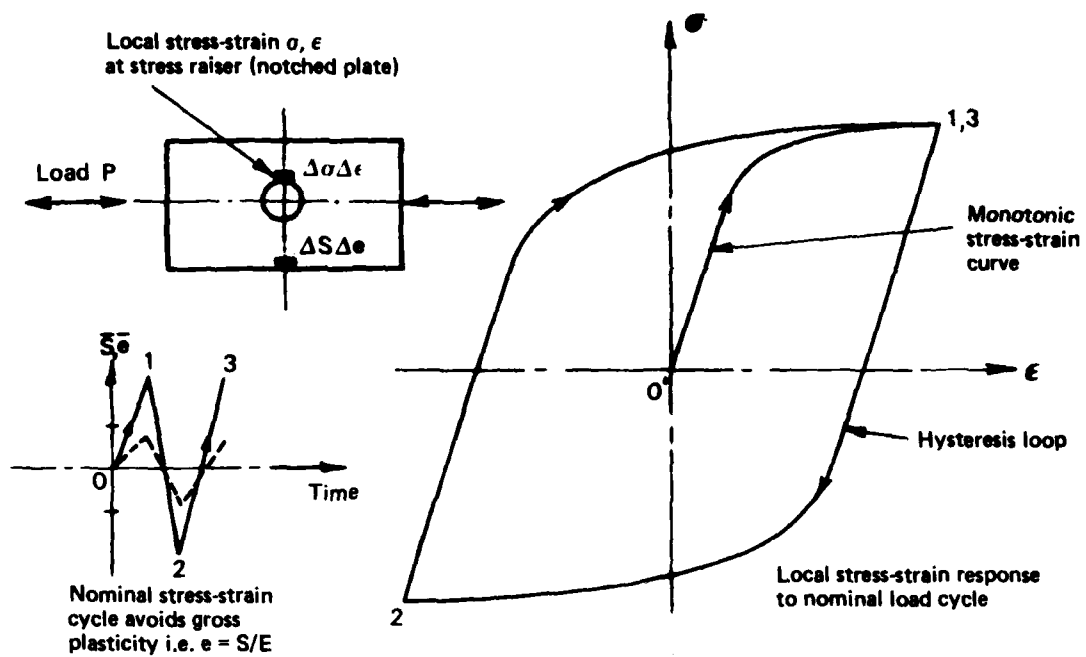


FIG. 2 HYSTERESIS OF LOCAL STRESS-STRAIN

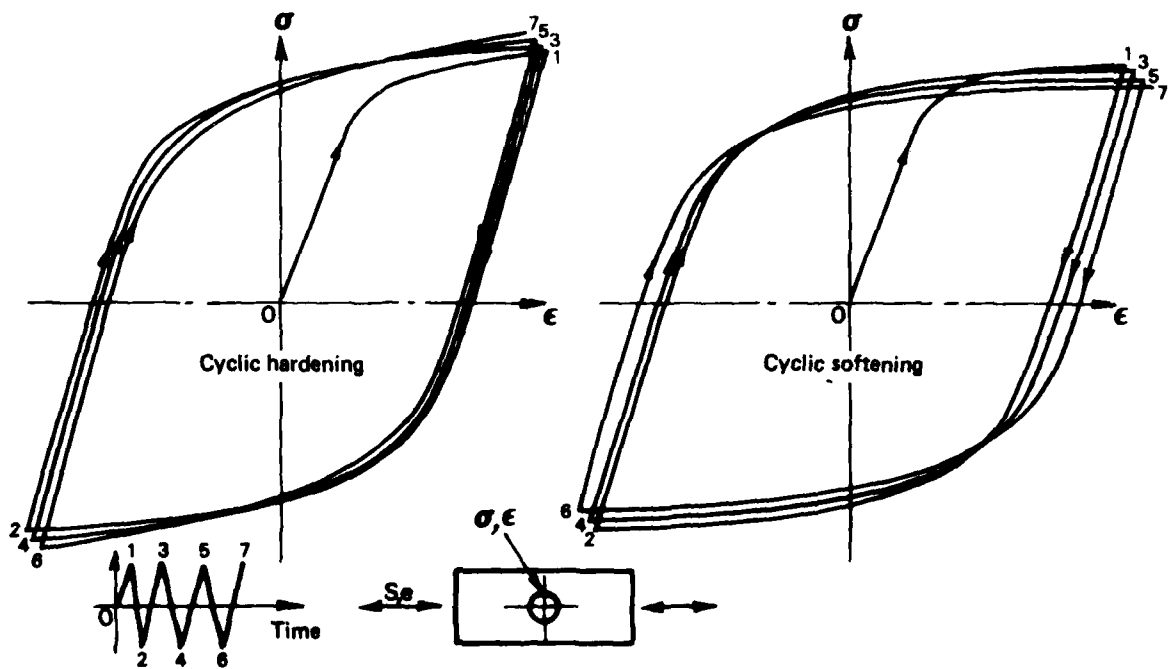


FIG. 3 CYCLE DEPENDENT HARDENING OR SOFTENING

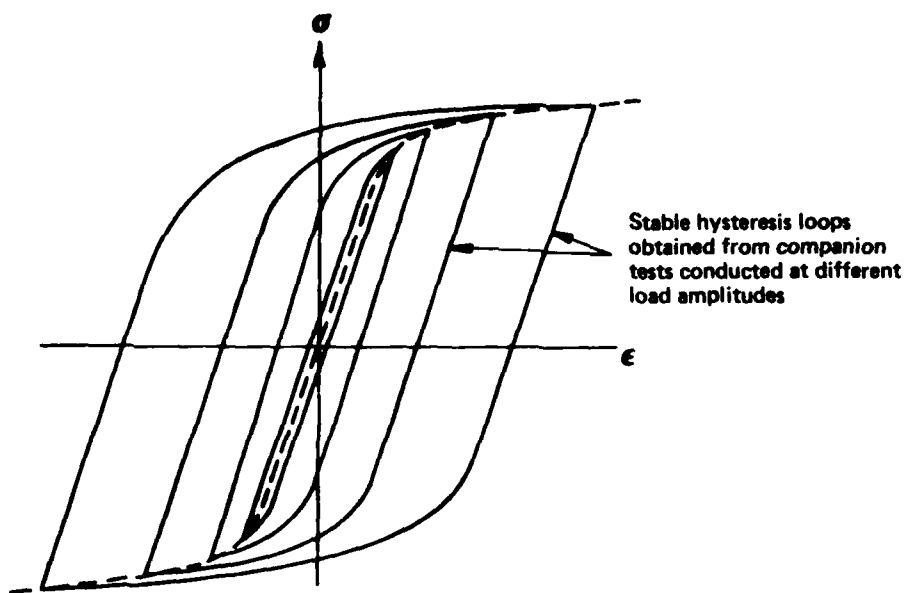


FIG. 4 THE CYCLIC STRESS-STRAIN CURVE

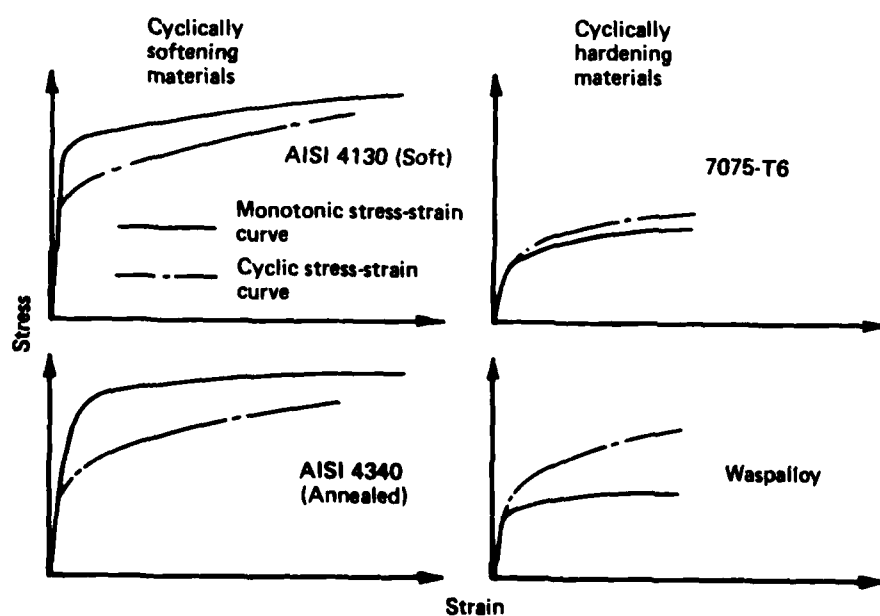


FIG. 5 MONOTONIC AND CYCLIC STRESS-STRAIN CURVES

Reference 11. Cyclic stress-strain data for a variety of metals is detailed in Reference 12. The law most commonly used to fit the cyclic stress-strain curve is similar to that used for monotonic curves, namely

$$\epsilon_t = \epsilon_e + \epsilon_p$$

$$\sigma = \frac{\sigma}{E} + \left(\frac{\sigma}{K'} \right)^{1/n'} \quad (1)$$

where ϵ_t = total strain,

ϵ_e = elastic strain,

ϵ_p = plastic strain,

σ = total stress,

E = Young's modulus,

K' = cyclic strength coefficient,

n' = cyclic strain hardening exponent.

The value of the cyclic strain hardening exponent is around 0.15 for most metals (a monotonic strain hardening exponent $n \approx n'$ will indicate that the metal cyclically hardens or vice versa).

Masing¹⁰ has shown that hysteresis loop shape can be related to the cyclic stress-strain curve by simply doubling both scales. Figure 6 illustrates this geometric similarity between a local stress-strain path and some segment from the start of the cyclic stress-strain curve.

Thus the total change of local strain in terms of local stress-increments is

$$\epsilon_t = \frac{\sigma}{E} + 2 \left(\frac{\sigma}{2K'} \right)^{1/n'} \quad (2)$$

which relates the hysteresis loop to the cyclic stress-strain curve using the co-ordinate system of Figure 7a, and parameters of the cyclic curve. Figure 7b shows the two curves joined as part of a loop. The starred quantities distinguish the two axis systems.

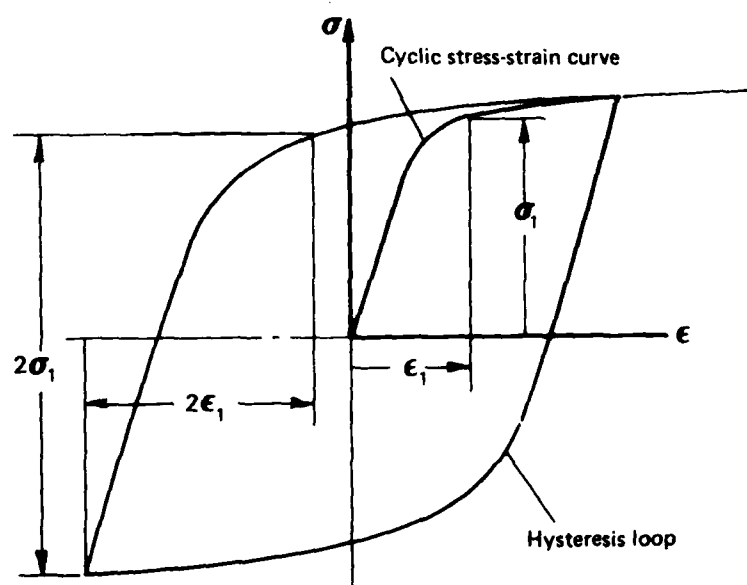


FIG. 6 MASING'S RULE — RELATION BETWEEN CYCLIC STRESS-STRAIN CURVE AND HYSTERESIS LOOP

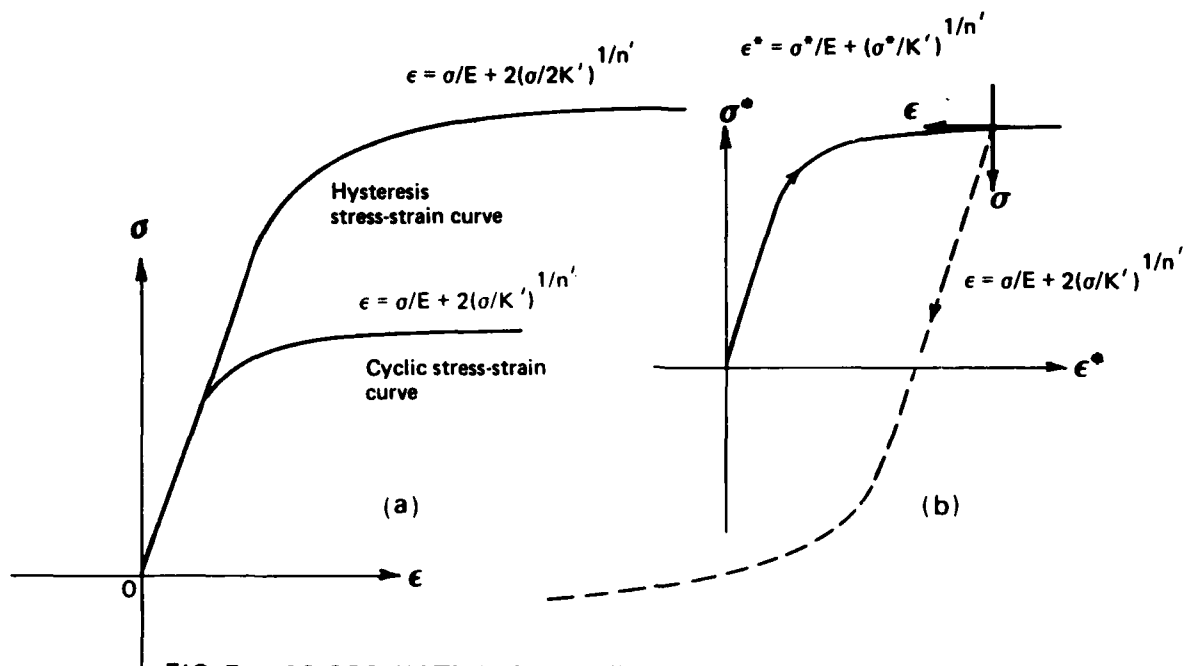


FIG. 7 CO-ORDINATE SYSTEM FOR HYSTERESIS STRESS-STRAIN CURVE

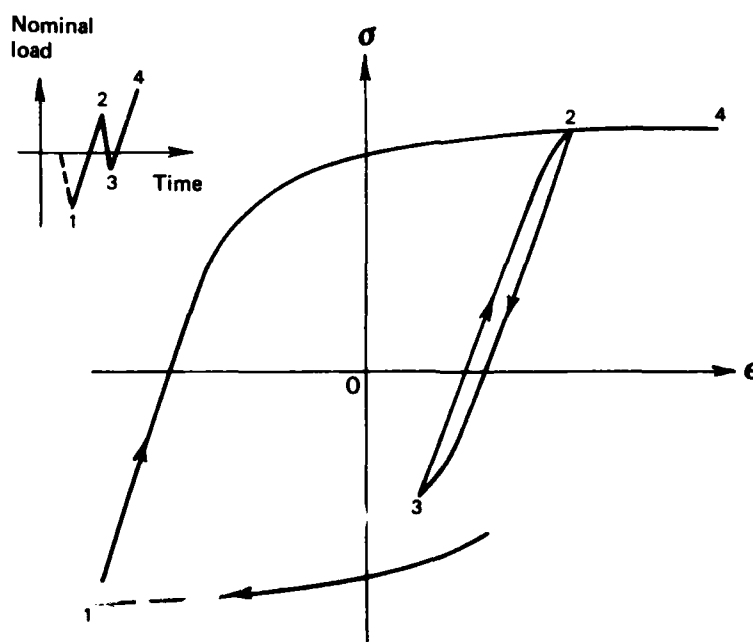


FIG. 8 CYCLIC MEMORY EFFECT

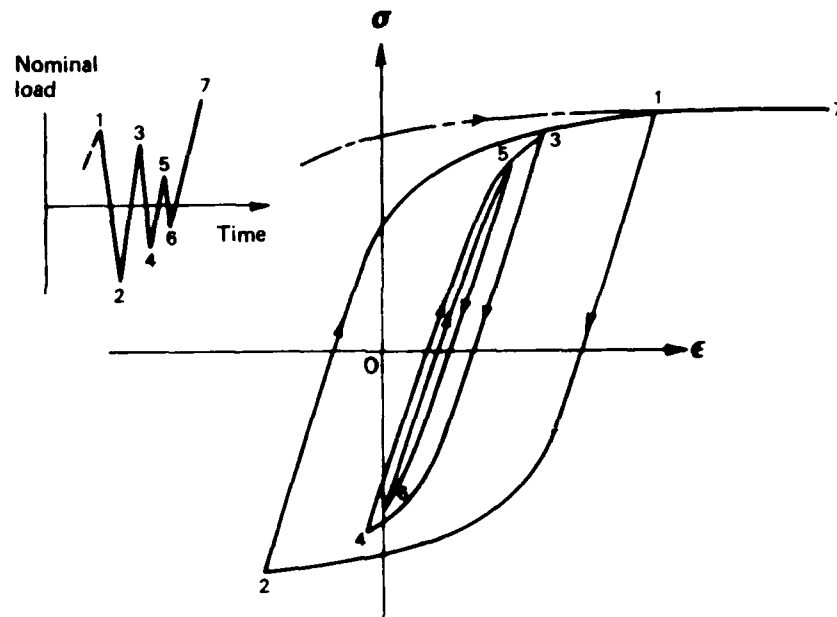


FIG. 9 COMPLEX MEMORY BEHAVIOUR

2.1 Memory

The next aspect of cyclic plasticity that needs to be considered is memory. Figure 8 demonstrates this for a metallic test specimen which has been strained in tension from condition 1 to condition 2 and then partially unloaded and loaded again. In deforming from condition 3 to 4 the metal remembers the prior deformation and deforms according to the initial response along 1 to 2. Under the asymptotic steady state the shape of the hysteresis (or memory) loop between 2 to 3 in Figure 8 is still described by (2) (there used twice). Even in compounded situations such as in Figure 9, where the local stress-strain state is moving from point 6 to 7 in response to the nominal load, change 6 to 7 remembers three prior deformation conditions.

2.2 Cyclic Relaxation and Creep

The last phenomena to be considered, cyclic relaxation of mean stress and cyclic creep under asymmetric loading can be demonstrated by strain-controlled testing in the first instance and by stress-controlled testing in the second. In Figure 10a the relaxation of mean stress towards zero in response to cycling between fixed local strain limits is clearly evident, likewise when the stress is controlled as in Figure 10b the local strain "creeps". Cyclic relaxation and cyclic creep represent essentially the same response (related to hardening and softening) under different control conditions and can be simulated by changing K' and n' in (2) during cycling. Material test data that permits the determination of the forcing functions $K'(N)$ and $n'(N)$, say to simulate cyclic relaxation and creep is sparse but it often leads to no significant change in life predictions.⁴⁻⁶

3. NEUBER NOTCH ANALYSIS

Neuber's analysis of stress and strain concentration in notched prismatic bodies in anti-plane shear has resulted in a state equation that is readily adapted to simulation of local stress-strains. In his paper Neuber shows that for this two-dimensional situation the geometrical mean of the stress and strain concentration factors under any arbitrary non-linear stress-strain law is equal to the Hookean stress concentration factor, i.e.

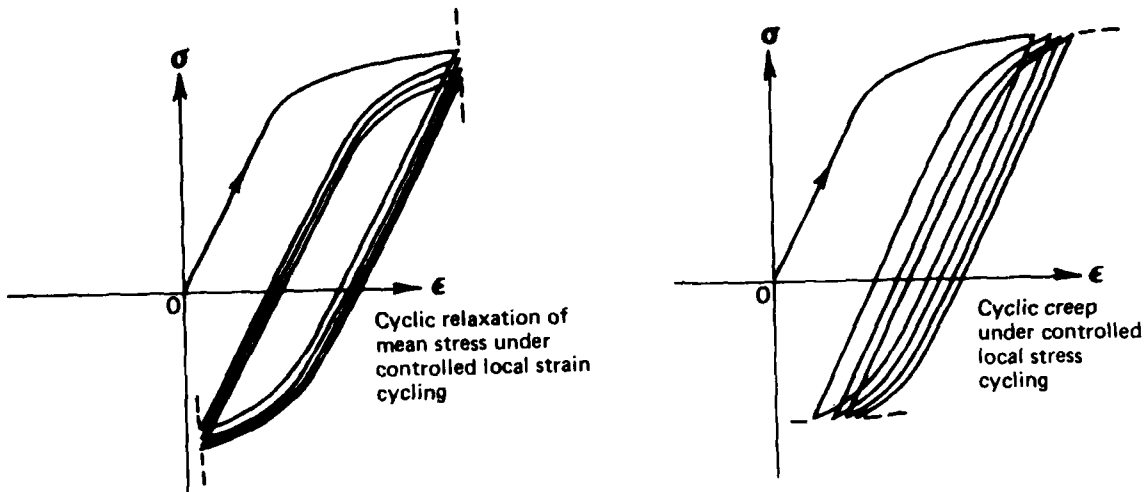


FIG. 10 REPRESENTATION OF CYCLIC RELAXATION AND CYCLIC CREEP

$$K_t = (K_\sigma K_\epsilon)^{1/2} \quad (3)$$

Topper *et al.*² have transcribed this equation to relate elastic change in nominal stress to change in local stress and strain as follows:

$$K_t = (K_\sigma K_\epsilon)^{1/2} \\ = \left(\frac{\Delta\sigma}{\Delta S} \frac{\Delta\epsilon}{\Delta e} \right)^{1/2} = \left(\frac{\Delta\sigma}{\Delta S} E \frac{\Delta\epsilon}{\Delta S} \right)^{1/2}$$

or

$$\Delta\sigma \Delta\epsilon = (K_t \Delta S)^2 / E. \quad (4)$$

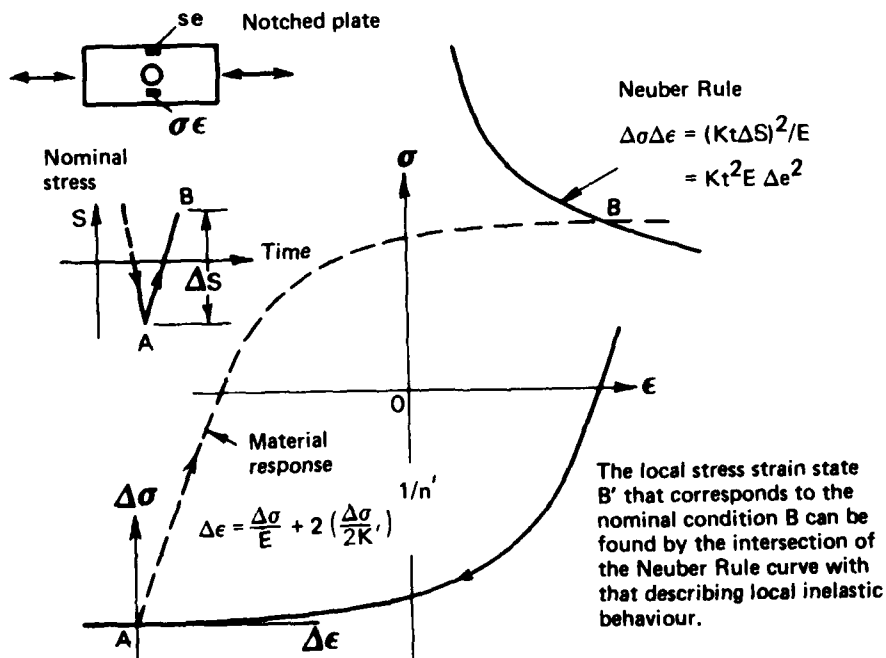


FIG. 11 NOTCH ANALYSIS USING NEUBER RULE

In this, σ and ϵ refer to local conditions while S and $e = S/E$ are nominal. Thus for a given change in nominal stress the changes in the local stress and strain will be related by the rectangular hyperbola (4). Several researchers^{1,12,14,15} realising that small sharp notches have less effect on fatigue life than indicated by K_t , have suggested that in such circumstances a modified factor K_f be used in lieu of K_t in (3) and (4). Called a fatigue strength reduction factor, it accounts for size effects and is used as a constant for a given material and geometry. Determination of K_f is discussed in References 2 and 28 but here we retain the notation K_t with this option understood.

Since most service load environments are recorded as nominal strain histories another appropriate form of (3) is

$$\Delta\sigma\Delta\epsilon = E K_t^2 (\Delta e)^2 \quad (5)$$

Equations (4) and (5) represent a stress-strain relation determined mainly by geometry. We have already mentioned in (2) another relation determined mainly by the material. Satisfaction of both these relations determines changes in stress and strain. Thus for a nominal stress or strain movement as in Figure 11, the resulting local stress-strain state will lie on the rectangular hyperbola defined by (4) or (5). The path along which the local state moves to that point will be appropriate to the characteristics of the material and its prior loading. Figure 11 illustrates this use of the Neuber rule in determining local stress-strain movement. For the particular case shown the material response curve is defined by the hysteresis function. If the material exhibits more complex behaviour such as memory effect as shown in Figure 12 then the local (and overall) stress-strain movement will be the intersection of the Neuber Rule and the material response curve that reflects the given conditions.

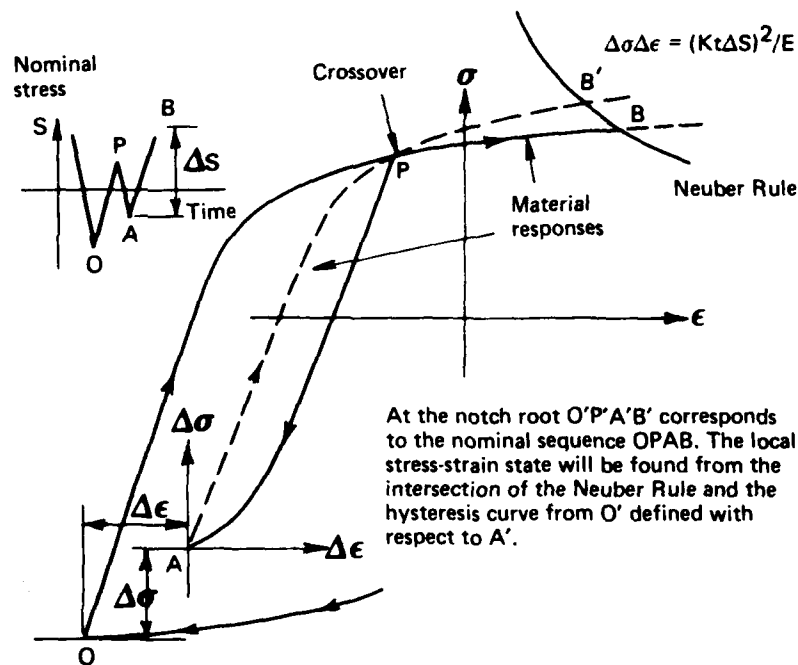


FIG. 12 COMPLEX LOCAL STRESS-STRAIN MOVEMENT USING THE NEUBER RULE
(A SINGLE MEMORY INFLUENCE IS ILLUSTRATED)

A mention of the limitations of Equations (3) to (5) is in order as there are constraints on their use. Firstly since (4) and (5) were derived assuming nominal stress to be always elastically related to nominal strain, they cannot be used when this is not so.

Secondly, as Neuber's analysis was based on the mathematics of two-dimensional antiplane shear, combined stress at a notch will not be adequately described by (3) nor subsequently Equations (4) and (5).

Finally, the equations apply only to the crack initiation phase of fatigue life; where crack propagation occupies a significant portion of the fatigue life, it must be predicted by fracture mechanics.

4. SIMULATION OF LOCAL STRESS-STRAIN

There are several different approaches to simulating the local stress strain response to a nominal load sequence.^{3,8,16,22,24,26,35} Martin *et al.* have developed a computer program that simulates local stress strain behaviour using a theoretical model built from combinations of springs and Newtonian frictional sliders. Wetzel⁸ and Conle¹⁶ later extended this approach using "push down lists" to control or more specifically activate the use of cyclic stress-strain data. For example the power law for monotonic or cyclic stress strain curves (i.e. Equations (1) and (2)) is approximated by a sequence of straight line segments which are used in constructing local stress-strain movements according to a vector of availability coefficients (the availability vector effectively stores the deformation history of the material). Cycle dependent hardening or softening and relaxation of mean stress or creep can be considered as small cycle-by-cycle changes of parameters in the cyclic stress strain curve quotation. As functions $K'(n)$ and $n'(N)$ these can be easily incorporated into a segmented representation of the stress-strain equation by altering the slopes of these segments appropriately. This approach has been utilised successfully by Wetzel and Conle and is amenable to various control conditions, e.g. simulating local stress strain behaviour of specimens subjected to controlled strain-cycling, controlled stress-cycling or Neuber rule controlled cycling (i.e. random loading).

4.1 Present Method

The simulation technique to follow differs from those of the references above as a result of a need to process random, nominal strain histories of unknown lengths. Thus the procedure had to be fast, use Neuber notch analysis as the control condition and be numerically stable—since Neuber control uses the existing local stress strain state to determine the next any inherent error in such a step is cumulative. Consequently the determination of a local stress-strain state should be done as quickly as possible, preferably in one step; hence the attraction of determining this state directly from the interaction of the appropriate hysteresis curve with the Neuber Control hyperbola as the fundamental operation of the model. Mathematically the state is the solution of (2) and (5), with appropriate origins, for $(\Delta\sigma, \Delta\epsilon)$.

4.1.1 Relaxation

Initially the simulation incorporated cyclic hardening softening and cyclic relaxation creep functions which modified K' and n' as appropriate though subsequently these phenomenon were deleted from the model as the marginal changes in life predictions that accompanied their use did not justify the penalties incurred with respect to program speed. (The sparsity of accurate data that permitted quantification of the parameters was also a problem.) Comprehensive validation of simulation models by Wetzel⁸ and Conle and Topper⁶ have suggested that it may unnecessary to include relaxation in most instances.

4.1.2 Modelling

Hence the basic simulation required only hysteresis and memory capability.

For this situation there exist only four basic types of movement in the local stress strain state and these are shown in Figure 13—movement along the cyclic curve 0-1, movement along

a hysteresis curve 3-4, movement which crosses from a hysteresis to a cyclic curve 1-2, and movement which crosses from one hysteresis curve to another hysteresis curve 6-3. Using these four movements any complex response can be built up using Neuber control.

Figure 11 shows Neuber control used to determine the end point of a local stress-strain movement corresponding to half a nominal load cycle. Because of the nature of the cyclic and hysteresis curves the solution B must be found by iteration.

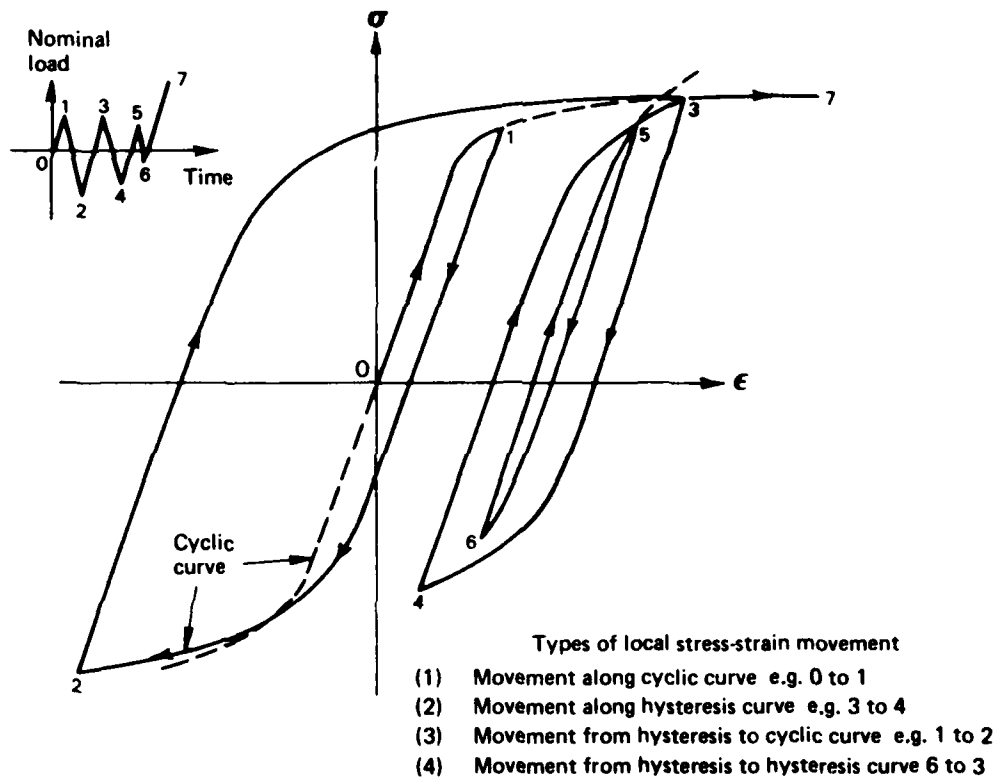


FIG. 13 CHARACTERISING LOCAL STRESS STRAIN MOVEMENT

4.1.3 Numerical Methods

Newton's method has been used in the implementing program since it combines speed with stability for functions like (2) and (5). The initial estimate of local stress is the exact solution of Neuber Control rule with the hysteresis equation without the elastic strain term. Thus $\Delta\sigma$ initially follows from

$$\Delta\epsilon_p = T_c \left(\frac{\Delta\sigma}{T_c K'} \right)^{1/n'}$$

where $T_c = 1$ for cyclic curve (type of curve: T_c).

$T_c = 2$ for hysteresis curve (type of curve: T_c).

The iteration to the solution from this initial estimate is quite rapid, even to high accuracy. There will be an error in determining point B in Figure 11 regardless of the simulation techniques, so that error control must be a feature of any Neuber based local stress-strain simulation.

In situations such as depicted in Figure 12 where a solution to an initial hysteresis curve and the Neuber control law is B' the Newton iteration does not stop. Since B' is found to exceed point P then a crossover is known to have occurred and the iteration starts again using B' as an estimate to the solution which is known to lie on the previous hysteresis curve. In complex memory behaviour the situation depicted in Figure 12 will occur repetitively with each successive solution used as an estimate for a further solution based on a more appropriate curve. This

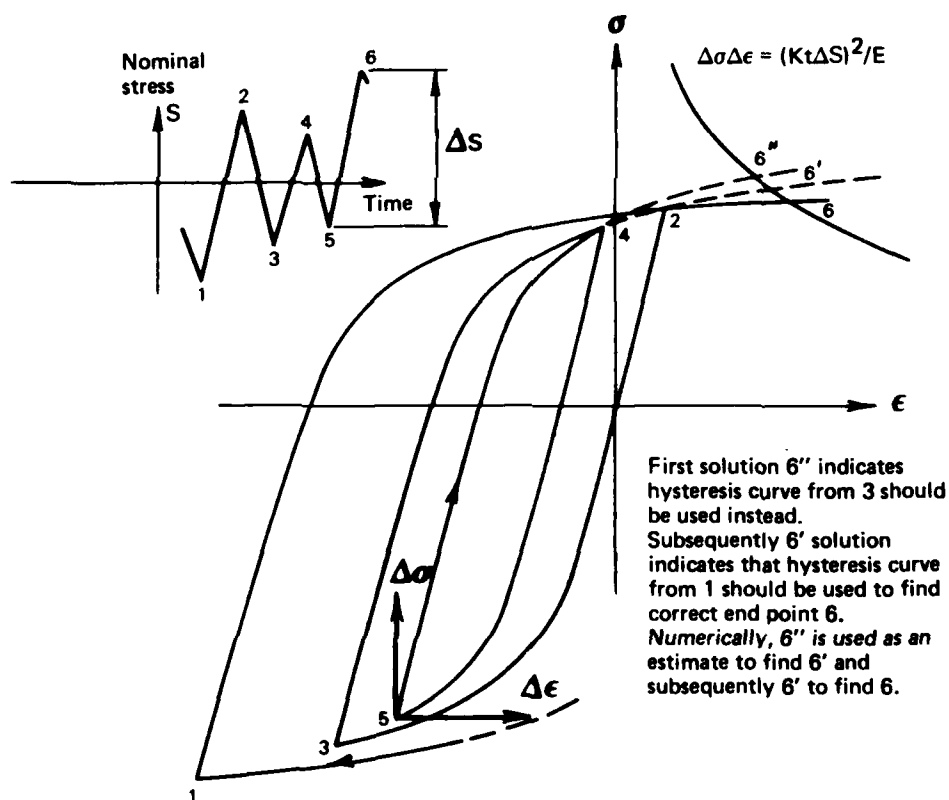


FIG. 14 ITERATION PAST SEVERAL HYSTERESIS CURVES

is shown in Figure 14 and although it may appear to involve extended and complex calculations the whole iteration to the correct solution is fairly direct within the program. (The hysteresis curves are expressed as general functions that represent also the cyclic curve as well as offset situations, e.g. the hysteresis curve OB in Figure 12 must be defined with respect to the origin A; the beginning of the current movement in the local stress-strain state) It should be pointed out here that although there may be several sets of iterations involved in determining a solution there is actually only one inherent error step. This is because intermediate solutions such as 6'' and 6' in Figure 14 are only required to determine the correct hysteresis curve. Only the accuracy of the last solution such as 6, will figure in the overall stability of the simulation during the processing of long histories.

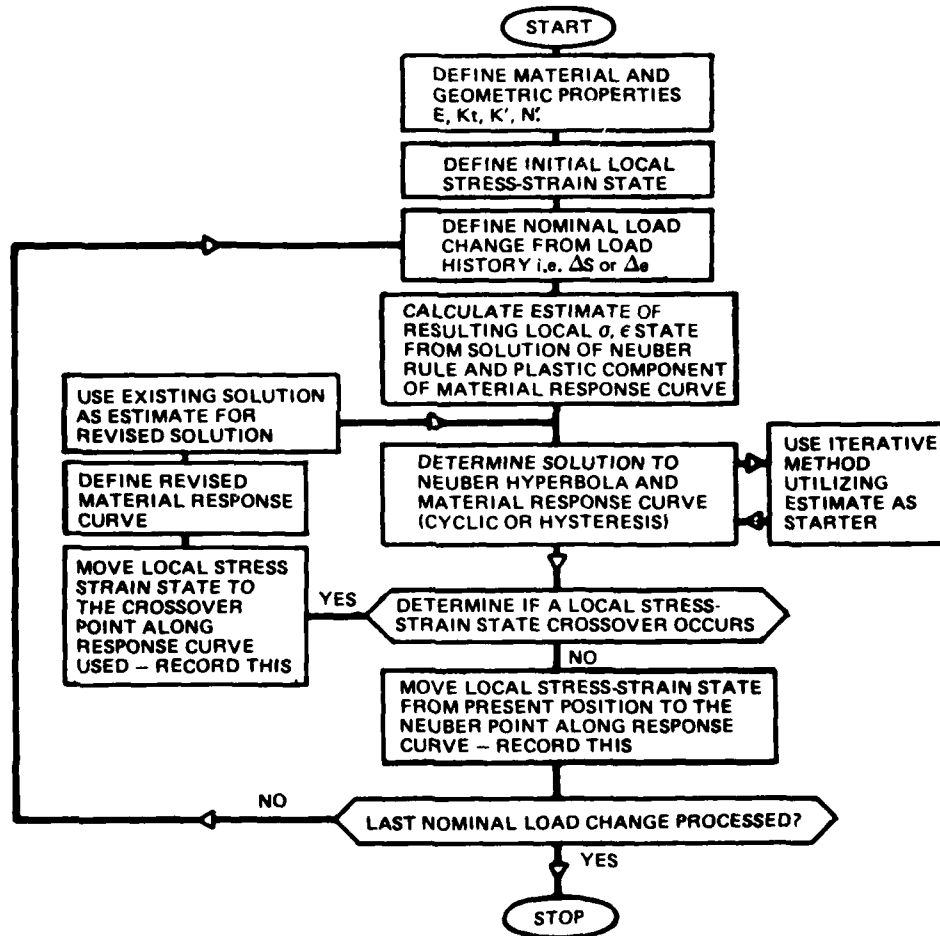


FIG. 15 FLOW CHART OF LOCAL STRESS-STRAIN SIMULATION

The flow chart of the simulation by the techniques described, is shown in Figure 15; and its implementation as a computer program is discussed in the Appendix.

Figure 16 shows a portion of a local stress-strain history simulated in the manner outlined from a service load history (nominal strain) measured close to a critical stress raiser. Hysteresis, memory and softening are evident, though as previously mentioned the capability for the last was subsequently considered unnecessary and removed from the model.

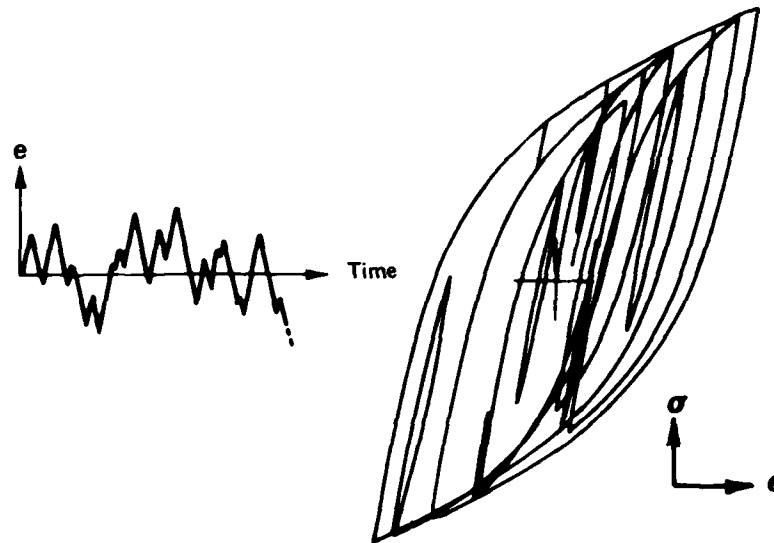


FIG. 16 A LOCAL STRESS-STRAIN HISTORY SIMULATED FROM NOMINAL STRAIN DATA USING THE NEUBER RULE

4.2 Miscellaneous Effects

In the Appendix it will be seen that small changes in the solution for (ϵ, σ) of (1) or (2) and (4) or (5) can lead to quite different program decisions. However, in a range-pair sense the differences arising thereby have only the same order of magnitude as these errors, this corresponding to different choices of turning points at nearly the same stresses.

In a similar way the accumulated error in a long sequence will most probably correspond to an erroneous mean load for the later range-pairs. This accumulated error may also appear on one of the large amplitude range-pairs. The reason for both these effects is that the conditions for the smaller range-pairs are likely to be satisfied over relatively few turning points while the larger range-pairs may well require the whole sequence for their completion. The error in range caused by drift obviously depends on the number of turning points between the defining peaks and this will probably be larger for large range-pairs.

The final solution of Equations (1) or (2) and (4) or (5), through the range-pair type of algorithm, depends uniquely on the immediately prior stress-strain state and another state further in the past. Thus each turning point is determined by two others. Intuitively one may imagine that satisfaction of range-pair conditions always corresponds to a closed hysteresis loop in the ϵ - σ plane. However, the mere dependence of each turning point upon two previous ones is not enough to guarantee this and some examples without closure have been found.

5. CALCULATION OF FATIGUE DAMAGE

Having translated a nominal load sequence into a local stress-strain sequence such as in Figure 16 it remains to resolve the damaging influence of the latter. The procedure used to accomplish this consisted of two steps:

- (1) cycle counting of the local stress-strain history;
- (2) determination of fatigue damage for each cycle produced by (1) and subsequent summation.

The cycle counting method used to process the local stress-strain histories was the range-mean-pair method²³ which counts cycles that relate to closed hysteresis loops. The algorithm that constitutes this method is very simple, very fast and counts in a single pass which allows it to be run in parallel with the simulation program. (The simulation model actually incorporates range-mean-pair detection logic within its own structure, though it is easier to discuss the two procedures separately. The logic is the same as that for selecting the proper hysteresis curve in solving for local stress-strain states.)

Subsequently, fatigue damage for each range-mean-pair cycle of local stress strain was determined using life data expressed as

$$N^\alpha \Delta \epsilon_p = C, \quad (6)$$

where N = no cycles to failure,

$\Delta \epsilon_p$ = plastic strain range for local strain cycles,

α, C = material parameters.

Equation (6) is commonly referred to as the Manson-Coffin Rule and it represents the linear relationship observed between the logarithms of the variables, i.e.

$$\log N = \alpha^{-1}(\log C - \log \Delta \epsilon_p). \quad (7)$$

Reference 12 contains cyclic life data for a range of common materials that allows estimation of the constants C and α in (6). In general $\alpha = 0.5-0.6$ whilst C is a small multiple of total strain to static failure. The damage sustained per range-mean-pair cycle is thus

$$1/N_i = (\Delta \epsilon_{pi}/C)^{1/\alpha}, \quad (8)$$

and for all the cycles in a sequence $1 \leq i \leq n$ the total damage is

$$D = \sum_{i=1}^n (\Delta \epsilon_{pi}/C)^{1/\alpha}. \quad (9)$$

Hence by combining the local stress-strain simulation procedure described in the previous section with the range-mean-pair cycle counting technique and linear accumulation of Manson-Coffin damage, a package is obtained which can be used for the fatigue analysis of any service load sequence.

It should be noted that though the linear cumulative damage law described above proved to be quite adequate in processing local stress-strain range-mean-pair cycles,^{2,5,6,7,8,13,18,20} it is thought that the inaccuracies that do exist in a simulation and damage calculation of this sort are due in the main to this linear rule,^{8,18} so that subsequent refinements would be best concentrated in this area.

6. CONCLUSIONS

The advantages of utilising cyclic stress-strain concepts in the fatigue analysis of service nominal stress histories have been well documented in the literature. An algorithm which utilises these concepts in the light of this experience has been described and its use in the analysis of fatigue environments should improve predictions of initial life. Its flexibility and fast analysis of the effects of mission changes, product improvements, load sequence, etc., should also be of value. It differs from similar programs by finding numerical solutions to the original Neuber and stress-strain or hysteresis relations without approximating the model. The logical steps in pairing a Neuber curve and a hysteresis curve for finding a stress-strain state transpire to be just the same

as those used in the stack inspection procedure²³ for range-pair counting. Since these are merely logical steps they cannot impair numerical accuracy. Because of this and because the model is not approximated the above method is particularly suitable for general, long, practical load sequences.

We have already noted that the application of Neuber analysis to the determination of local stress-strain was such that subsequent fatigue damage analysis was relevant to crack initiation only, and that where crack propagation formed a large portion of total life an extended analysis should be used to incorporate crack growth. The use of a strain-based intensity factor solution for the initiation and growth of short cracks from notches is detailed by Haddad *et al.*²⁷ and by combining this with local stress-strain/damage analysis as described in the present paper, considerable scope exists for developing a general fatigue program.

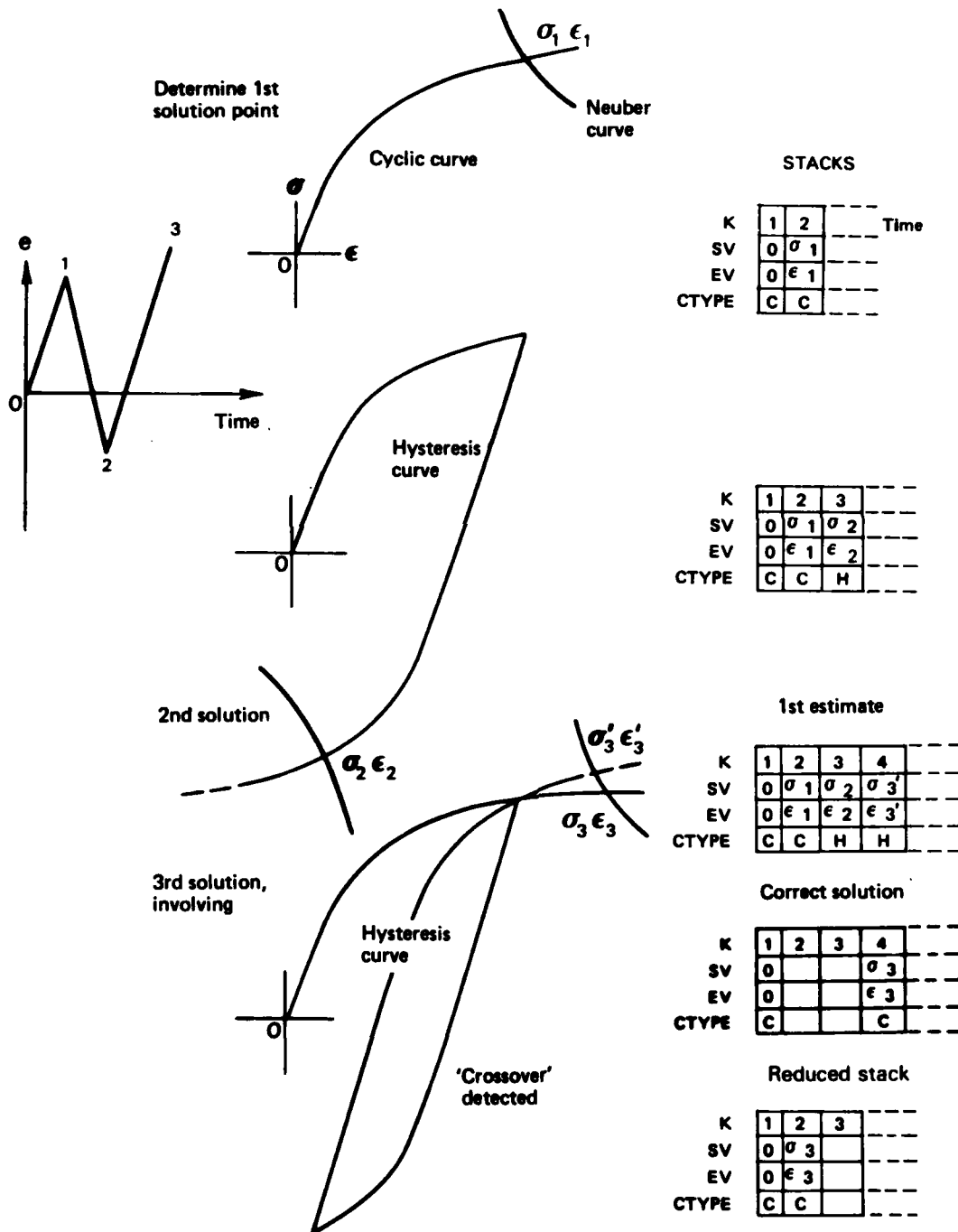


FIG. 17 OPERATION OF LOCAL STRESS-STRAIN STACKS

REFERENCES

1. Neuber, H.—Theory of stress concentration for shear strained prismatic bodies with arbitrary non-linear stress-strain law. *J. of Applied Mech.*, December 1961.
2. Topper, T. H., Wetzel, R. M., and Morrow J.—Neuber's rule applied to fatigue of notched specimens. *J. of Mat.*, Vol. 4, No. 1, March 1969.
3. Morrow, J., Wetzel, R. M., and Topper, T. H.—Laboratory simulation of structural fatigue behaviour. ASTM STP 462, 1970.
4. Wetzel, R. M.—Smooth specimen simulation of fatigue behaviour of notches. *J. of Mat.*, Vol. 13, No. 3, 1968.
5. Martin, J. F., Topper, T. H., and Sinclair, G. M.—Computer-based simulation of cyclic stress-strain behaviour with applications to fatigue. *Mat. Research and Standards*, MTRSA Vol. 11, No. 2.
6. Conle, A., and Topper, T. H.—Sensitivity of fatigue life predictions to approximations in the representation of metal cyclic deformation response in a computer-based fatigue analysis model. 2nd Int. Conf. Structural Mechanics in Reactor Technology, Berlin, September 1973.
7. Socie, D. F.—Fatigue life prediction using local stress-strain concepts. *Exp. Mech.*, February 1977.
8. Wetzel, R. M.—A method of fatigue damage analysis. Ph.D. Thesis, Dept. of Civil Eng., University of Waterloo, Ontario, Canada, 1971.
9. Dowling, N. E.—Fatigue failure predictions for complicated stress-strain histories. ASTM *J. of Mats.* Vol. 7, pp. 71-87, 1972.
10. Masing, G.—*Proc. Second Int. Cong. of App. Mech.*, Zurich, 1926.
11. Landgraf, R. W.—Determination of the cyclic stress-strain curve. *J. of Mat.*, Vol. 4, No. 1, March 1969.
12. Smith, R. W., Hirschberg, M. H., and Manson, S. S.—Fatigue behaviour of materials under strain cycling in low to intermediate life range. NASA Tech. Note D-1574.
13. Topper, T. H., and Conle, F. A.—An approach to the analysis of non-linear deformation and fatigue response of components subjected to complex service level histories. *Proc. of Inter. Symp. of Exp. Mech.*, University of Waterloo, Canada, 1972.
14. Leis, B. N., and Topper, T. H.—Assessing notch strength reduction in cyclically loaded notched components. *Proc. 2nd Int. Conf. on Structural Mech. in Reactor Technology*, Vol. 5, Berlin 1973.
15. Gowda, C. U. B., Leis, B. N., and Smith, K. N.—Dependence of fatigue notch factor on plasticity and duration of crack growth. ASTM *J. of Test & Eval.*, 1974.
16. Conle, F. A.—A computer simulation assisted statistical approach to the problem of random fatigue. M.Sc. Thesis, University of Waterloo, Canada, 1974.
17. Landgraf, R. W., and La Pointe, N. R.—Cyclic stress-strain concepts applied to component fatigue life prediction. SAE paper 740280.
18. Schütz, D., and Gerharz, J. J.—Critical remarks on the validity of fatigue life evaluation methods based on local stress-strain behaviour. *Cyclic Stress-Strain and Plastic Deformation Aspects of Fatigue Crack Growth*. ASTM STP No. 637, Philadelphia, Pa. 1977, pp. 209-233.

19. Morrow, J.—Cyclic plastic strain energy and fatigue of metals. ASTM STP 378, June 1964.
20. Popov, E. P., and Petersson, H.—Cyclic metal plasticity: experiments and theory. ASCE 140 No. EM6, December 1978.
21. Conle, A., Nowack, H., and Hanshmann, D.—The effect of engineering approximations on fatigue life evaluation for variable amplitude loading. *Problems with fatigue in Aircraft, Proceedings of the eighth ICAF Symposium*, Lausanne, 2-5th June 1975. Swiss Federal Aircraft Establishment (F+W) CH-6032 Emmen, Switzerland.
22. Potter, J. M. *et al.*—A user's manual for the sequence accountable fatigue analysis computer program. USAF Flight Dynamics Laboratory, Wright-Patterson AFB, Ohio, May 1974.
23. Fraser, R. C.—A one-pass method for counting range-mean-pair cycles for fatigue analysis. Aeronautical Research Laboratories, Structures Note 454, 1978.
24. Fatigue life estimation under variable amplitude loading. ESDU Data Sheet 77004.
25. Estimation of endurance and construction of constant amplitude SN curves from related data corrected for notch and mean stress effects. ESDU Data Sheet 76014.
26. Generalization of smooth continuous stress-strain curves for metallic material. ESDU Data Sheet 76016.
27. Haddad, M. H., Smith, F. N., and Topper, T. H.—A strain based intensity factor solution for short fatigue cracks initiating from notches. *ASTM: Proc. of 11th National Symposium on Fracture Mechs*, 1978.
28. Buch, A.—Fatigue Strength Calculation Methods. *Technion Israel Institute of Technology*, TAE 314, September 1977.

APPENDIX

Computer Simulation of Local Stress-Strain

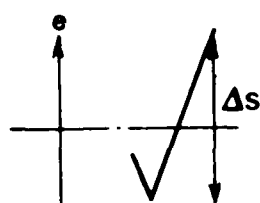
Because of its powerful decision constructs the language PASCAL was used for the program of the local stress-strain simulation flow-charted in Figure 15. Denoted LSSF (Local Stress-Strain Follower) the program was divided into four modules:

- (1) the function *CURVE* which determined the strains on the hysteresis (or cyclic) and Neuber curves corresponding to a given stress value as passed to it by
- (2) the function *NP*, containing a procedure based on Newton's method, which upon receipt of an estimate to the stress at the solution, where the material response curve, either the hysteresis or cyclic curves, intersects the Neuber curve) iterates towards the solution until a specified relative error is obtained;
- (3) the procedure *MOVE* which controls the output of results, i.e. the local stresses and strains corresponding to input nominal stresses and strains;
- (4) the main program which tracks the local stress-strain path incorporating the basic movements as depicted in Figure 13.

The fundamental operator of the range-mean-pair method²³—the turning point stack—was used in this program for similar reasons. A method of storing local stress-strain turning points was needed so that decisions about "cross-overs" could be made. Figure 9 indicates, theoretically at least, that every local stress-strain turning point in a history may have to be retained throughout a simulation: when the local stress-strain state moves in response to the load change 6 to 7 it jumps out of three loops and information on each of these loops (i.e. points 6, 5, 4, 3, 2, 1) is required to currently determine the point 7. Thus stacks *SV[K]*, *EV[K]* and *CTYPE[K]* denoting respectively local stress stack of *K* elements, local strain stack of *K* elements and the type of movement to *SV[K]* and *EV[K]* ("C" for cyclic curve and "H" for hysteresis curve) were used to contain each local stress-strain turning point and the nature of the movement involved. When closed hysteresis loops are detected the corresponding elements of the stacks are emptied and the gaps closed. In this way the stacks are continually loaded and emptied in response to local stress-strain movements. This may be recognized as an exact analogy of the operation of the turning point stack of Topper and Conle¹³.

Figure 17 depicts a simple local stress-strain movement using the stacks. The third stack shows the first approximation to the stress-strain point *SV[4]*, *EV[4]*, corresponding to σ'_θ , ϵ'_θ . After the third stack a hypothetical fourth stack has been added which shows the values σ_θ and ϵ_θ , the solution of correct equations derived from previous history and the first approximations (see Figure 18). In the fifth stack the now established hysteresis loop σ_1 , σ_2 has been removed. In practice the program proceeds directly from the third stack to the fifth.

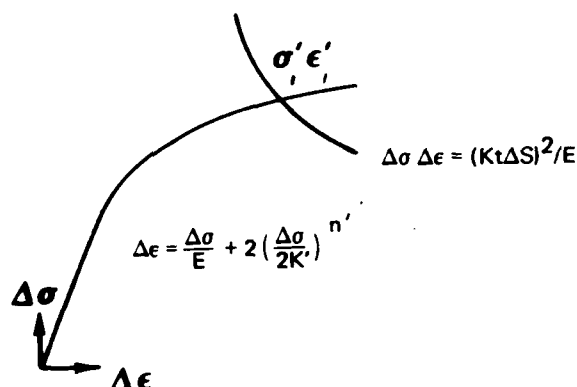
The main decision of the program upon calculation of a solution point is to determine if a "cross-over" occurs and if so which type. This reduces to establishing whether the previous point lies on either a cyclic or hysteresis curve and then whether the present point has crossed to the outside of this previous curve. Figure 18 illustrates the total simulation broken down into all possible movements that occur within the scope of the concepts outlined previously. It should be noted that although absolute stresses and strains are ultimately determined the solution of a given material response using Neuber, is determined with respect to the immediately preceding local stress-strain state, i.e. the local stress-strain co-ordinates implied by the Neuber equation as depicted in Figure 11 are used. Decisions about equality of real numbers must be made with regard to a relative error criterion, e.g. two stresses or strains may be considered equal if they differ by less than 0.005%.



Consider the local stress-strain response that may result from the Kth nominal load application ΔS (the prior local history has been determined and is contained in the stacks SV, EV, CTYPE).

- (1) An estimate of the response is made using the material hysteresis curve. The stacks are altered accordingly:

i.e. $SV[K] = \sigma'$
 $EV[K] = \epsilon'$
 $CTYPE[K] = "H"$



- (2) This response is checked against prior material behaviour using CTYPE. For CTYPE $[K - 1] = "C"$, i.e. previous point lies on cyclic curve, three movement types are possible:

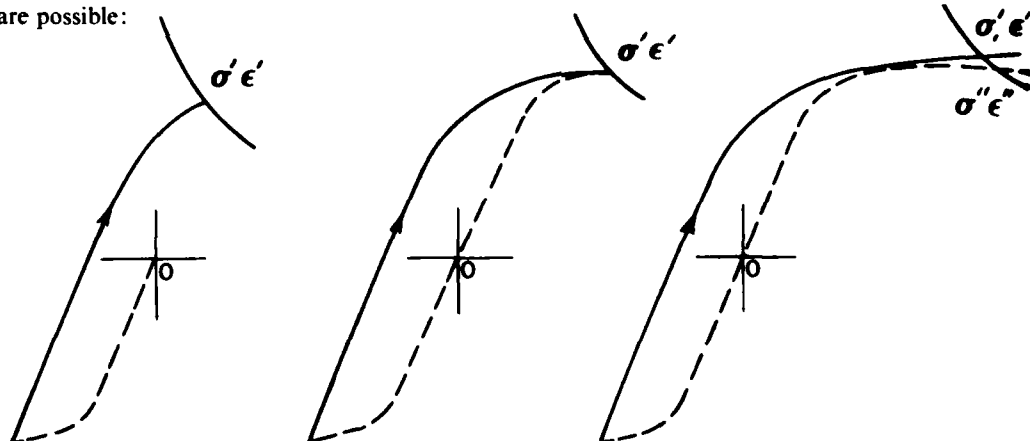


FIG. 18 PROGRAM DECISIONS AND RESULTING LOCAL STRESS-STRAIN STATE MOVEMENTS

$ SV[K] < SV[K - 1] $	$ SV[K] = SV[K - 1] $	$ SV[K] > SV[K - 1] $
$SV[K] = \sigma'$	$SV[K] = \sigma'$	$SV[K] = \sigma''$
$EV[K] = \epsilon'$	$EV[K] = \epsilon'$	$EV[K] = \epsilon''$
$CTYPE[K] = "H"$	$CTYPE[K] = "C"$	$CTYPE[K] = "C"$

(Crossover from hysteresis curve must occur. Correct point σ'' , ϵ'' determined using cyclic curve.)

For $CTYPE[K - 1] \neq "C"$, that is, the previous point lies on a hysteresis curve, the resulting movement will depend on $SV[K - 2]$ and $CTYPE[K - 2]$. For example let

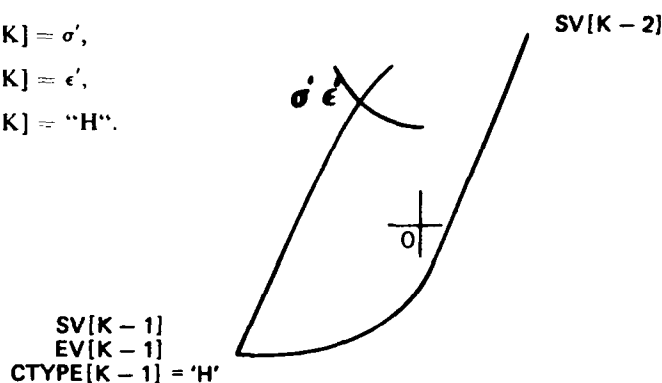
$$TEST = SV[K] - SV[K - 1]$$

Then for $TEST = 0$ the movement is such that

$$SV[K] = \sigma',$$

$$EV[K] = \epsilon',$$

$$CTYPE[K] = "H".$$



Otherwise for $TEST > 0$ two movements are possible:

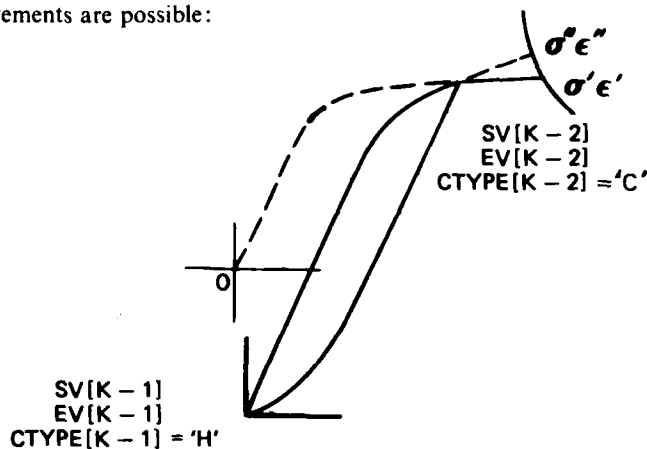
- (i) $CTYPE[K - 2] = "C"$

Stress-strain state moves from hysteresis curve to cyclic curve as shown:

$$SV[K] = \sigma',$$

$$EV[K] = \epsilon'$$

$$CTYPE[K] = "C".$$



- (ii) $CTYPE[K - 2] \neq "C"$.

Stress-strain state moves from hysteresis curve to hysteresis curve.

For complex memory situations involving a movement out of many loops the local state may eventually jump out of cyclic curve, i.e. movements according to (i) above only occur at the end of this movement.

Note that contents of stack are overwritten as in Figure 17 when loops are closed by a movement in state.

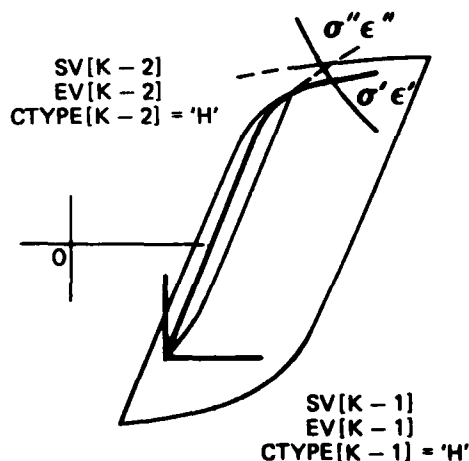


FIG. 18 PROGRAM DECISIONS AND RESULTING LOCAL STRESS-STRAIN STATE MOVEMENTS (contd.)

DISTRIBUTION

Copy No.

AUSTRALIA

Department of Defence

Central Office

Chief Defence Scientist	1
Deputy Chief Defence Scientist	2
Superintendent, Science and Technology Programs	3
Australian Defence Scientific and Technical Representative (UK)	—
Counsellor, Defence Science (USA)	—
Defence Central Library	4
Joint Intelligence Organization	5
Document Exchange Centre, D.I.S.B.	6-22

Aeronautical Research Laboratories

Chief Superintendent	23
Superintendent—Structures Division	24
Structures Divisional File	25
Author: R. C. Fraser	26
J. M. Finney	27
L. R. Gratzner	28
C. King	29
V. Romeo	30
W. Harch	31
D. G. Ford	32
G. S. Jost	33
A. D. Graham	34
J. Q. Clayton	35
R. Nethercott	36
Library	37

Materials Research Laboratories

Library	38
---------	----

Defence Research Centre, Salisbury

Library	39
---------	----

Central Studies Establishment Information Centre

Library	40
---------	----

Engineering Development Establishment

Library	41
---------	----

Defence Regional Office

Library	42
---------	----

RAN Research Laboratory		
Library		43
Navy Office		
Naval Scientific Adviser		44
Army Office		
Army Scientific Adviser		45
Royal Military College, Library		46
Air Force Office		
Air Force Scientific Adviser		47
DGAIRENG		48
Engineering (CAFTS) Library		49
HQ Support Command (SENGSO)		50
Department of Productivity		
Government Aircraft Factories		
Library		51
Mr. M. Cameron		52
Department of Transport		
Secretary		53
Library		54
Airworthiness Group: Mr. R. Douglas		55
Mr. C. Torkington		56
Statutory, State Authorities and Industry		
CSIRO Mechanical Engineering Division, Chief		57
CSIRO Materials Science Division, Director		58
Qantas, Library		59
Trans-Australia Airlines, Library		60
Ansett Airlines, Library		61
BHP Melbourne Research Laboratories		62
Commonwealth Aircraft Corporation, Library		63
Commonwealth Aircraft Corporation, Mr. R. C. Beckett		64
Hawker de Havilland Pty. Ltd. (Librarian), Bankstown		65
Universities and Colleges		
Adelaide	Barr Smith Library	66
Deakin	Library	67
	Dr. B. Bathgate	68
Flinders	Library	69
James Cook	Library	70
La Trobe	Library	71
Melbourne	Engineering Library	72
	Engineering, Dr. J. Williams	73
Monash	Library	74
	Prof. I. J. Polmear, Materials Eng.	75
Newcastle	Library	76
New England	Library	77
New South Wales	Physical Sciences Library	78
	Prof. Trail-Nash, Structural Eng.	79
Sydney	Engineering Library	80
	Prof. G. A. Bird, Aeronautical Eng.	81

Queensland	Engineering Library	82
Tasmania	Engineering Library	83
	Prof. R. A. Oliver, Civil & Mech. Eng.	84
Western Australia	Library	85
RMIT	Library	86
	Mr. H. Millicer, Aeronautical Eng.	87
	Mr. Pugh, Mechanical Eng.	88
CANADA		
	Aluminium Labs. Ltd., Library	89
	CAARC Co-ordinator (Structures)	90
	NRC, National Aeronautical Establishment, Library	91
	NRC, National Aeronautical Establishment, Div. of Mech. Eng. (Dr. D. McPhail)	92
Universities		
McGill	Library	93
Toronto	Institute of Aerophysics	94
Waterloo	Dept. of Mech. Eng.: Prof. L. F. Topper	95
	Dr. D. J. Burns	96
FRANCE		
	ONERA, Library	97
	Service de Documentation, Technique de l'Aeronautique	98
	Mr. W. Barrois	99
GERMANY		
	LBF, Dr. D. Schutz	100
	DVLR, Dr. W. Schutz	101
INTERNATIONAL COMMITTEE ON AERONAUTICAL FATIGUE		
	Per Australian Representative, G. S. Jost	102-126
INDIA		
	CAARC Co-ordinator, Structures	127
	Civil Aviation Department, Director	128
	Defence Ministry, Aero, Development Est., Library	129
	Indian Institute of Science, Library	130
	Indian Institute of Technology, Library	131
	National Aeronautical Laboratory, Director	132
ITALY		
	Associazione Italiana di Aeronautica e Astronautica, Prof. Evla	133
	Fiat Co., Dr. G. Gabrielli	134
	Universita Degli Studi di Pisa, Dr. A. Salvetti	135
ISRAEL		
	Technion-Israel Institute of Technology	
	Prof. J. Singer	136
	Prof. A. Buch	137
JAPAN		
	National Aerospace Laboratory, Library	138
Universities		
	Tokyo Institute of Space and Aerospace, Library	139
	Tohoku (Sendai), Library	140

Research Institute of Strength and Fracture of Materials:	
Prof. Yamanaka	141
Prof. T. Yokobori	142
M. Ichikawa	143
Kobe, Prof. T. Nakagawa	144
Kyushu Institute of Technology, Library	145
NETHERLANDS	
Central Org. for Applied Science	146
National Aerospace Laboratory	147
NEW ZEALAND	
Defence Scientific Establishment, Librarian	148
Transport Ministry, Civil Aviation Division Library	149
Canterbury University, Library	150
SWEDEN	
Aeronautical Research Institute, Dr. Sigge Eggwertz	151
Chalmers Institute of Tech. Library	152
Kungl. Tekniska Hogskolens	153
SAAB-Scania, Library	154
SWITZERLAND	
F & W Ltd.	155
UNITED KINGDOM	
CAARC, Secretary	156
Aeronautical Research Council	157
Royal Aircraft Establishment:	
Farnborough, Library	158
Bedford, Library	159
CATC Secretariat	160
British Library:	
Science Reference Library	161
Lending Division	162
Fulmer Research Institute Ltd., Research Director	163
Science Museum Library	164
Welding Institute Library	165
National Engineering Laboratories, Superintendent	166
Naval Construction Research Establishment, Superintendent	167
CAARC Co-ordinator, Structures	168
Aircraft Research Association, Library	169
British Ship Research Association	170
Central Electricity Generating Board	171
Motor Industries Research Association, Director	172
Rolls Royce:	
Aeronautics Division, Library	173
Bristol Siddeley Division, Library	174
British Aerospace Corporation:	
Kingston-Borough Division	175
Manchester Division	176
Kingston-upon-Thames, Headquarters Library	177
Weybridge-Bristol Division	178
Warton Division	179
British Hovercraft Corporation Ltd., Library	180
Short Brothers & Harland	181
Westland Helicopters Ltd.	182

Universities and Colleges

Bristol	Library, Engineering Department	183
Cambridge	Library, Engineering Department	184
London, Queen Mary College	Library, Department of Aeronautics	185
Manchester	Library, Engineering	186
Nottingham	Library	187
Southampton	Library	188
Strathclyde	Library	189
Cranfield Inst. of Technology	Library	190
Imperial College	The Head	191
	Prof. of Mechanical Engineering	192
	Library, Department of Aeronautics	193

UNITED STATES OF AMERICA

NASA Scientific and Technical Information Facility	194
Sandia Group Research Organisation	195
American Institute of Aeronautics and Astronautics	196
Applied Mechanics Reviews	197
The John Crerar Library	198
US Atomic Energy Commission, Division of Tech. Information	199
Cessna Aircraft Co., Executive Engineer	200
Battelle Memorial Institute:	
Library	201
Dr. D. Broek	202
Metals Abstracts	203
Air Force Flight Dynamics Labs., Wright-Patterson AFB	204
NASA, Langley (Virginia), John Crews Jr.	205
National Bureau of Standards, Library	206
US Dept of Transportation, Transportation Systems Center,	207
Dr. Elaine Savage	
US Naval Research Laboratory, Washington, DC	208
Calspan Corporation	209

Universities and Colleges

Brown	Prof. R. E. Meyer	210
Brooklyn	Library, Polytechnic Aero. Lab.	211
California Inst. of Technology	Library, Graduate Aero. Lab.	212
	Dr. M. Holt, Dept. of Aeronautics	213
Florida	Mark H. Clarkson, Dept. of Aero. Eng.	214
Harvard	Library, Engineering	215
Illinois	Dept. of Theoretical and Applied Mechanics	216
Iowa State	Dr. G. K. Sekory, Mechanical Eng.	217
Johns Hopkins	Dept. of Mechanical Engineering	218
Massachusetts Inst. of Technology	Library	219
New Mexico	Dept. of Nuclear Engineering	220
Pennsylvania	Library, School of Engineering	221
Stanford	Library, Department of Aeronautics	222
Wisconsin	Memorial Library, Serials Department	223

Spares**224-233**

**DATE
FILMED**

4-8